colloids and interfaces

MDPI

Article

Fluctuations in Humidity Influence the Structure Formation and Swelling of Casein Microparticles

Calvin Hohn and Ronald Gebhardt *

Faculty of Mechanical Engineering, RWTH Aachen University, Chair of Soft Matter Process Engineering (AVT.SMP), Aachen 52062, Germany; calvin.hohn@rwth-aachen.de
* Correspondence: ronald.gebhardt@avt.rwth-aachen.de

Abstract: Caseins are a sustainable alternative to non-biodegradable materials for the production of functional microparticles. These show a characteristic swelling behavior when they are prepared from micellar casein under gentle conditions using depletion flocculation and subsequent film drying. The typical two-step swelling process is a result of the internal particulate network structure, which is surrounded by water channels. The seasonal and daily fluctuations in humidity during the 16 h film drying process influence the structure formation and swelling kinetics, which we analyze using system dynamics analysis. Microparticles with better and more uniform swelling properties can be produced using a drying apparatus with an integrated humidifier and ventilation system. At higher humidity levels, the casein micelles are less compressed during film drying, which facilitates the initial swelling of the microparticles. Furthermore, the more stable drying conditions in the drying apparatus result in a more homogeneous compaction of the film, which causes similar swelling rates for different microparticles.

Keywords: air humidity; casein microparticles; film drying; swelling; system dynamics modeling

Citation: Hohn, C.; Gebhardt, R. Fluctuations in Humidity Influence the Structure Formation and Swelling of Casein Microparticles. *Colloids Interfaces* **2024**, *8*, 45. https://doi.org/10.3390/colloids8040045

Academic Editors: Georgi G. Gochev and Reinhard Miller

Received: 7 June 2024
Revised: 29 July 2024
Accepted: 8 August 2024
Published: 14 August 2024

1. Introduction

Caseins can be used as a sustainable alternative to non-biodegradable materials for the production of functional microparticles. Caseins have a flowable, naturally open structure [1]. In nature, they occur as spherical association colloids with average sizes of 200 nm [2,3]. These so-called casein micelles are held together by electrostatic contacts between caseins and colloidal calcium phosphate nanoclusters, as well as by hydrophobic and other physical interactions between the caseins [4–6], while steric stabilization is provided by k-casein, which is distributed unevenly as a polyelectrolyte brush on the surface [7]. A recent model description of casein micelles as a sponge-like structure [8] can also explain the compaction and deformation of casein micelles during film drying [9]. Casein micelles are highly hydrated with 3.4 g of water per g casein [10]. Most of the water is trapped in the porous casein micelle structure, while a smaller part is bound to caseins or associated with the κ-casein surface layer [11].

There is currently great interest in functionalizing caseins as a transport platform for bioactive substances [12]. Both micro- and nanocapsules have been produced from casein, and biologically active agents, probiotic cells and nutraceuticals have been encapsulated [13]. However, there is still a great need for research to understand the behavior of the wall material casein, from which these capsules are made, under different physicochemical conditions [14]. The investigation of the size changes of the caseins in different media is of particular importance with regard to the function of the particles. For example, the swelling of microparticles plays a significant role in the immobilization of enzymes for biosensors or in the controlled release of bioactive substances [15–17]. A key challenge is to produce the capsules under conditions that preserve the activity of the encapsulating substance. We have developed a gentle process for the production of microparticles

from casein aggregates, which are produced by depletion flocculation at neutral pH and subsequent film drying under ambient conditions [18]. The casein aggregates are formed from the casein micelles due to the volume exclusion of pectin, which is added in a specific mixing ratio at pH 7 [19]. It has recently been shown that these aggregates are also retained after acidification. Liquid yogurt is formed in this case because no continuous network is formed [20]. The aggregates deform in shear and extensional flows and disintegrate when pectin is removed. However, the aggregates solidify during a film drying step and remain stable after preparation from the film matrix [21]. During drying, the increase in concentration of the casein micelles within the aggregates leads to deviations from the hard sphere behavior, deformation and finally to a liquid–solid transition, which is accompanied by a structural arrest [22,23]. Only this step stabilizes the casein aggregates, which is in contrast to other casein microparticle preparations where drying processes are used. In these cases, spray or freeze-drying processes followed after stable structure formation of casein utilizing ionotropic gelation and cross-linking, coacervation, or enzymatic gelation with transglutaminase or chymosin [16,24–27].

The casein microparticles (CMPs) produced in this way swell in an alkaline milieu in a two-step process and finally disintegrate. The two-step kinetics can be attributed to the multi-level structure of the CMPs. Their inner structure consists of 1–2 µm large building blocks, which are composed of several casein micelles. The first swelling step leads to the expansion of the caseins within the casein micelles and building blocks. In contrast, the second swelling step concerns the interactions between the micelles within the building blocks. These are weakened as a result of prolonged swelling, which finally causes the irreversible disintegration of the CMPs [28]. The expansion process at pH 11 takes place over a period of several minutes and is particularly suitable for studying the swelling properties and stability of differently structured CMPs [21]. Swelling-induced decomposition can be prevented, for example, by subsequent chemical crosslinking via disulfide bridges [29].

During the two-step swelling of CMPs, we observed large variations in the rates. It is generally known that, in addition to the amino acid sequence, constant environmental conditions in the cell are also crucial for the synthesis of functional proteins [30]. For the artificially produced CMPs, the drying conditions during compaction of the film could have a significant influence on the structural and functional properties. The mechanical properties in the film state depend in particular on the relative humidity during production, storage and use, as has been shown for the example of caseinate films [31]. Humidity fluctuations affect the water content in the films and thus influence the structuring processes of the protein network [32]. Our hypothesis is therefore that more uniform humidity levels during the film drying step will lead to CMPs with more uniform swelling properties. As the relative humidity in the laboratory is subject to seasonal and daily fluctuations, we also prepare CMPs in a drying apparatus that reduces the fluctuations over the 16 h drying process. To test the influence of absolute humidity, we prepare CMPs on two days, one month apart, and analyze the swelling properties of the CMPs compared to those dried in air on the laboratory bench.

2. Materials and Methods

2.1. Materials and Preparation Process of Casein Microparticles

Hydrochloric acid (1 M), potassium hydroxide (>90%), sodium hydroxide (1 M) and pectinase from Aspergillus niger were purchased from Merck (Merck, Darmstadt, Germany). Micellar casein concentrate powder MC80 was supplied by Milei GmbH, Leutkirch, Germany. Highly methylated citrus pectin (CU 201, DE° > 70%) was provided by Herbstreith & Fox (Herbstreith & Fox GmbH & Co. KG, Neuenbürg, Germany). All salts for the preparation of simulated milk ultrafiltrate (SMUF), as well as BisTris methane, calcium chloride and sodium dodecyl sulphate were purchased from VWR, Darmstadt, Germany. All solutions were prepared with Milli-Q water from the laboratory water purification system (Simplicity UV System, Merck, Darmstadt, Germany).

SMUF buffer was prepared according to the method described by Dumpler et al. by dissolving all required salts stepwise in Milli-Q water with constant stirring [33]. Sodium azide was also added to the SMUF buffer at a concentration of 0.5 g/L to inhibit the growth and activity of microbiological organisms. The pH was finally adjusted to 6.7 with KOH solution.

For a pectin solution (2%), 2 g of citrus pectin was dissolved in 98 g of BisTris buffer solution. To dissolve the pectin completely, the mixture was stirred vigorously at 80 °C for 3 h. It was then cooled to 20 °C and the pH of the pectin solution was adjusted to 6.8 with NaOH solution.

To produce a casein dispersion with a final concentration of 7.36% casein, 5 g of MC80 powder was added to 45 g of SMUF solution. The casein solution was stirred for 1 h at room temperature, then for 4 h at 4 °C and then for a further hour at 37 °C at 400 rpm in each case. The pH value of the casein solution was 6.7. A pectinase solution with an enzyme activity of ≈36 units/mL was used for film hydrolysis. For this, 0.47 mL of pectinase was added to 10 g of buffer.

Figure 1 summarizes the main process steps of CMPs manufacture. First, casein aggregates were formed by depletion flocculation [19,34]. For this, the micellar casein solution and pectin were mixed in a ratio of 3 to 0.3 wt% under neutral pH conditions. The formed casein aggregates were then compacted by film drying and solidified into stable microparticles [18]. For this purpose, 3.9 g of the solution was distributed on glass Petri dishes (Ø 70 mm) and drying was carried out both on the laboratory bench and in a drying apparatus at T = 22 °C.

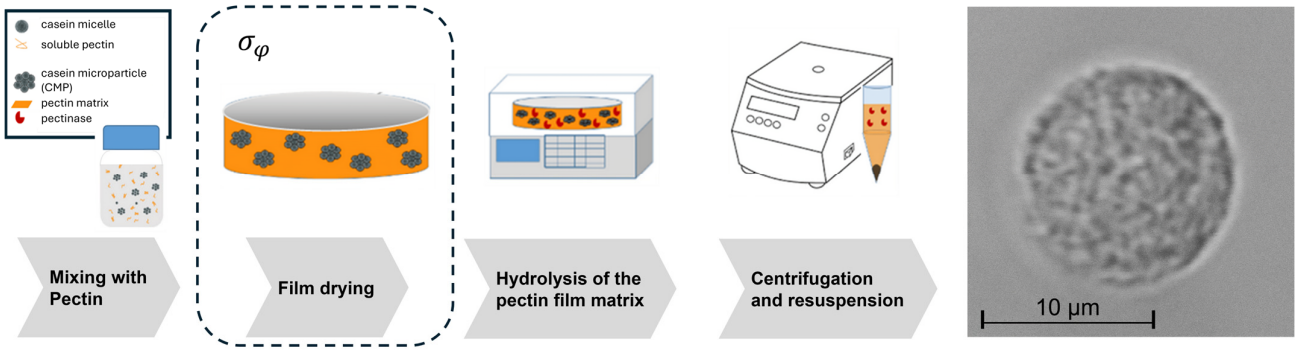

Figure 1. Schematic illustration of the four main process steps in the manufacture of CMPs from casein micelles by depletion flocculation. The drying step with the humidity variation, σ_φ as an influencing variable is highlighted in a frame. A representative CMPs with a typical internal microstructure is shown on the right.

In the apparatus, the air flow (indicated by red arrows in Figure 2) was directed over three levels to ensure drying under more uniform humidity conditions. The humid air reached the second level via a humidifier (HU450, AIRROBO, Singapore) placed on level I with an adjustable fog volume flow (125, 190, and 300 mL/h). Supported by two fans (computer fan d = 120 mm, max. 2000 rpm, UNYKAch, Getafe, Madrid, Spain), it reached level III through an adjustable gap, where it flowed over the films in Petri dishes. A wireless sensor (TP357, ThermoPro, Carrum Downs, VIC, Australia) was placed inside the third level of the apparatus behind the Petri dishes to record the relative humidity data.

Both film preparations were dried for 16 h at varying humidity. The microparticles were then isolated from the dried pectin matrix by enzymatic hydrolysis. This was performed by adding 10 mL of pectinase solution (37 units/mL in buffer solution) to the Petri dish and performing the hydrolysis in a ThermoMixer (Eppendorf, Eppendorf AG, Hamburg, Germany) with continuous shaking (160 rpm) at 47 °C for 2 h. The supernatant solution was then mixed with the pectinase solution. The supernatant solution containing the microparticles was then collected and centrifuged (at T = 22 °C and 1500 RCF for 10 min).

The CMPs in the sediment were separated from supernatant and finally resuspended in BisTris buffer.

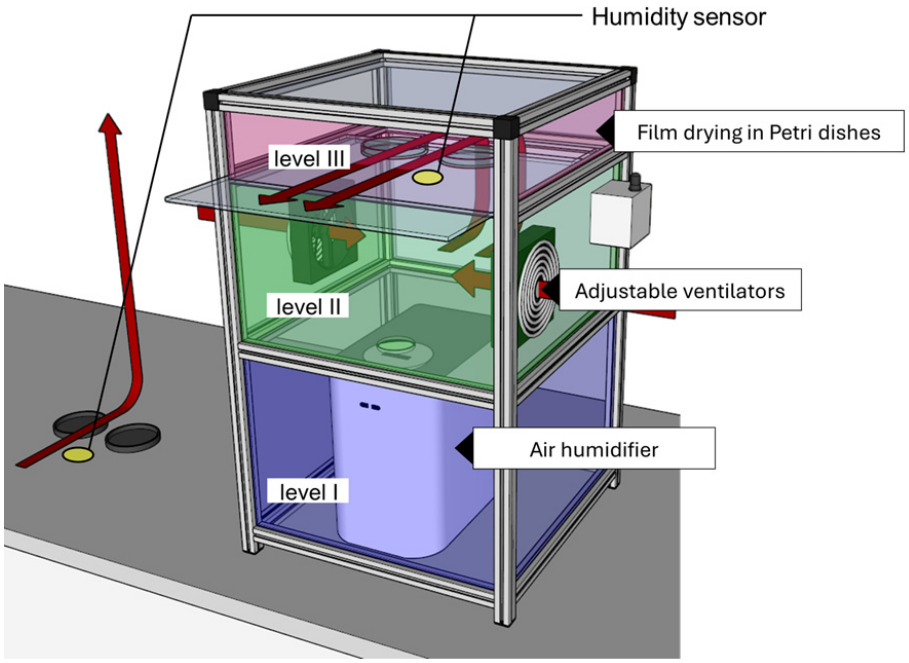

Figure 2. Schematic illustration of drying on the laboratory bench and in the drying apparatus, where the air supplied by a humidifier (level I) is directed through two diagonally arranged, adjustable ventilators on level II over the film preparations, i.e., Petri dishes on level III.

2.2. Swelling Experiments

The swelling of individual CMPs was investigated microscopically in 3D-printed flow-through cells with a sieve cell design [21]. To ensure diffusion of the CMPs into the sieve quenchers, the sieve cells were not moved for 10 min after filling. The flow cell was then placed under a Leica DMIL LED inverse microscope (Leica Microsystems, GmbH, Wetzlar, Germany) equipped with a Basler camera (Basler AG, Ahrensburg, Germany) and connected to a syringe pump (Harvard Apparatus, Holliston, MA, USA) via a PHD ULTRA™ polyethylene tube (Ø 0.55 mm). A flow rate of 0.07 mL per minute was selected for the exchange of the medium in the sieve cell with medium (ultrapure water, adjusted to pH 11). In addition, Thymol blue dye (Carl Roth GmbH + Co. KG Karlsruhe Germany) was added to the exchange medium in order to determine the exact start time of the swelling with the camera system.

The swelling of the microparticles in the sieve holes was recorded with a Basler camera using Basler video recording software version 1.3 (Basler AG Ahrensburg Germany) at a rate of 2 frames per second for 45 min. The images were extracted with PyCharm (version 2021.1.3, JetBrains, Prague, Czech Republic) and the projection areas of the CMPs were calculated with ImageJ software Version 1.53t (Wayne Rasband public domain USA).

2.3. System Dynamics Modeling and Simulation

The dynamic model to simulate the two-step swelling kinetics of the CMPs was created using Stella 1.6 software (iseesystems.com, Lebanon, NH, USA). The underlying flow diagram is shown in Figure 3. The spherical reservoir volume is filled by two volume flows that are activated at different times. The rate of volume change of the reservoir,

$$\frac{dV}{dt} = \sum_{i=1,2} RC_i \cdot \sigma_t^i \cdot curr\ Vol, \quad (1)$$

depends on a rate coefficient, RC_i, and the current filling volume of the reservoir, currVol, for each of the two volume flows. The rate coefficients RC_i, are calculated using step functions at the characteristic times as follows:

$$\sigma_t^i = \begin{cases} 0 \; for \; t < time_i \\ 1 \; for \; t \geq \; time_i \end{cases} \tag{2}$$

The differential equation, Equation (1), was solved numerically using Euler's integration method with a step size of 0.25 s. The particle area, A, was then calculated using the following spherical approximation and optimally adjusted by iteration:

$$A_t = \frac{3 \cdot V_t}{4 \cdot R_t} \tag{3}$$

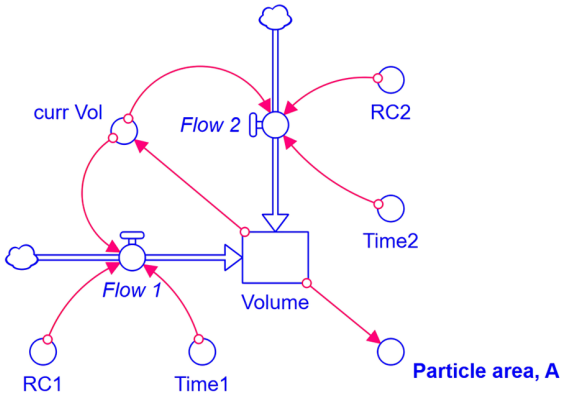

Figure 3. Stella model for the simulation of the two steps swelling curves of CMPs at pH 11. The particle area is calculated from the particle volume, which swells due to two volume flows, *Flow 1* and *Flow 2*. These depend on the current volume and a rate coefficient RC, which is activated at a characteristic time.

3. Results and Discussion

We studied the influence of different drying conditions on the swelling of CMPs. For this purpose, drying was carried out both on the laboratory bench, as in previous studies, and in a newly developed drying apparatus (see Figure 2).

Figure 4 shows the change in relative humidity on a preparation day both on the laboratory bench and in the drying box during the entire drying process. The relative humidity of the outside air measured by the local weather station near the place of investigation is also shown for comparison. The humidity remained almost constant at 96% during the entire drying process. The humidity on the laboratory bench fluctuated greatly depending on the time of day and showed a maximum relative humidity difference of approx. 9% during the 16 h drying period. In contrast, the humidity in the box did not follow this trend and stabilized at a value of 41% after approx. 5 h. The overshooting effect in the first 5 h can be explained by the comparatively large amount of moisture that escapes from the suspension at the beginning. After 5 h, a film has formed and the fluctuations in relative humidity are reduced. Within the film, the fragile casein aggregates are pressed together and solidified by the shrinking film matrix. This leads to an increase in the concentration of casein micelles within the aggregates and to deviations from the hard sphere behavior, deformation and finally to a liquid–solid transition, which is accompanied by a structural arrest [22,23]. The formation of spherical, stable CMPs takes a total of 16 h. CMPs formed by hydrolysis of the film matrix after shorter drying times are highly deformed, fragile and have a high tendency to aggregate (see Figure 4, right panel).

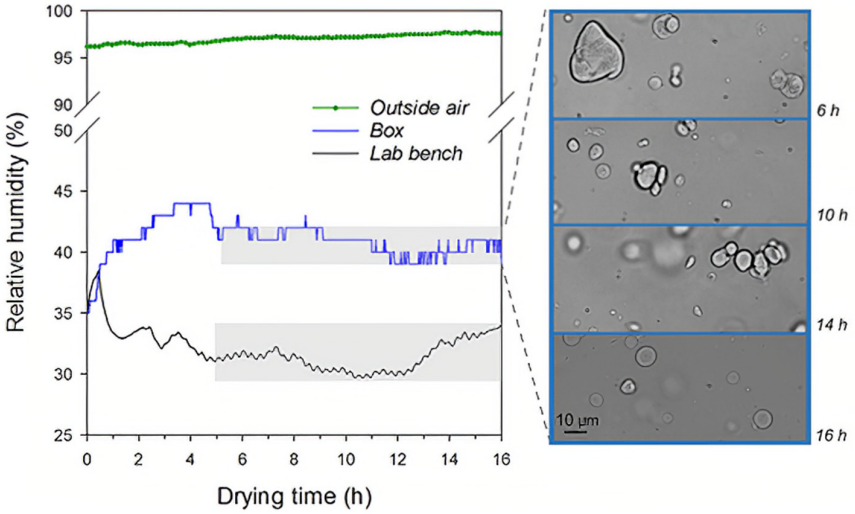

Figure 4. Fluctuations in air humidity during the drying processes. Fluctuations in humidity in the outside air, as well as in the box and on the laboratory bench, during the drying processes (left panel) and structural ripening of the CMPs with increasing drying times.

A total of two CMPs preparations were carried out one month apart. One part of the sample was dried in air under laboratory conditions and the other part in the drying apparatus described above. Three CMPs were selected from each preparation and their swelling was analyzed at pH 11. For this purpose, flow-through cells with a sieve cell design were used, which allow the microscopic observation of the swelling of individual CMPs after a medium exchange [21]. By exchanging the medium, a pH shift from pH 6.7 to pH 11 was induced, which triggered the swelling process. Figure 5 shows the changes in particle area relative to the initial area as a function of swelling time for all particles investigated. The start time of the swelling kinetics was determined using the Thymol blue indicator by means of a color change, which was detected by the camera system. A typical two-step swelling process was observed for all CMPs. The individual swelling steps are almost linear, as shown by the lines for the swelling kinetics of two differently dried CMPs in Figure 5. The swelling process ended within 30 min with the complete disintegration of the particles, which was previously reported for swelling at pH 11 [21]. The disintegration occurred after the particles had swollen to two to five times their initial particle area and thus in a range described in a study with a large sample size under these conditions [35]. However, the swelling kinetics for the CMPs produced in the drying apparatus (red symbols) were much closer together than those traditionally dried on the laboratory bench (black symbols). For both types of drying (laboratory bench and box), the CMPs from May (open symbols) showed stronger swelling than the particles from April (closed symbols).

We analyzed all swelling curves from Figure 5 with the system dynamics model shown in Figure 3 to investigate this finding in more detail. This model is based on the observation that the spherical shape of the CMPs is maintained during the swelling process until shortly before decomposition [35]. Furthermore, it is assumed for the balance (Equation (1)) that the increase in volume is due to volume flows from the surrounding medium and that there are no sources and sinks for the particle volume. Sinks and sources could occur, for example, because of changes in the solvent density in combination with the solvation of exposed surfaces or changes in the void volume in combination with the folding state of the proteins [36]. However, bound water represents only a small fraction, as most of it is trapped in the porous structure of the casein micelle [11]. Furthermore, due to the lack of a tertiary structure and the rheomorphic, open structure of caseins [1], volume changes due to swelling-induced conformational changes can probably be neglected. The two-step swelling kinetics are described by two volume flows, each of which depends on the current volume of the CMPs, as well as a rate coefficient *RC1* or *RC2* and the associated

characteristic times. The particle area is then calculated using the spherical approximation from the particle volume, which is obtained by numerical integration of Equation (1).

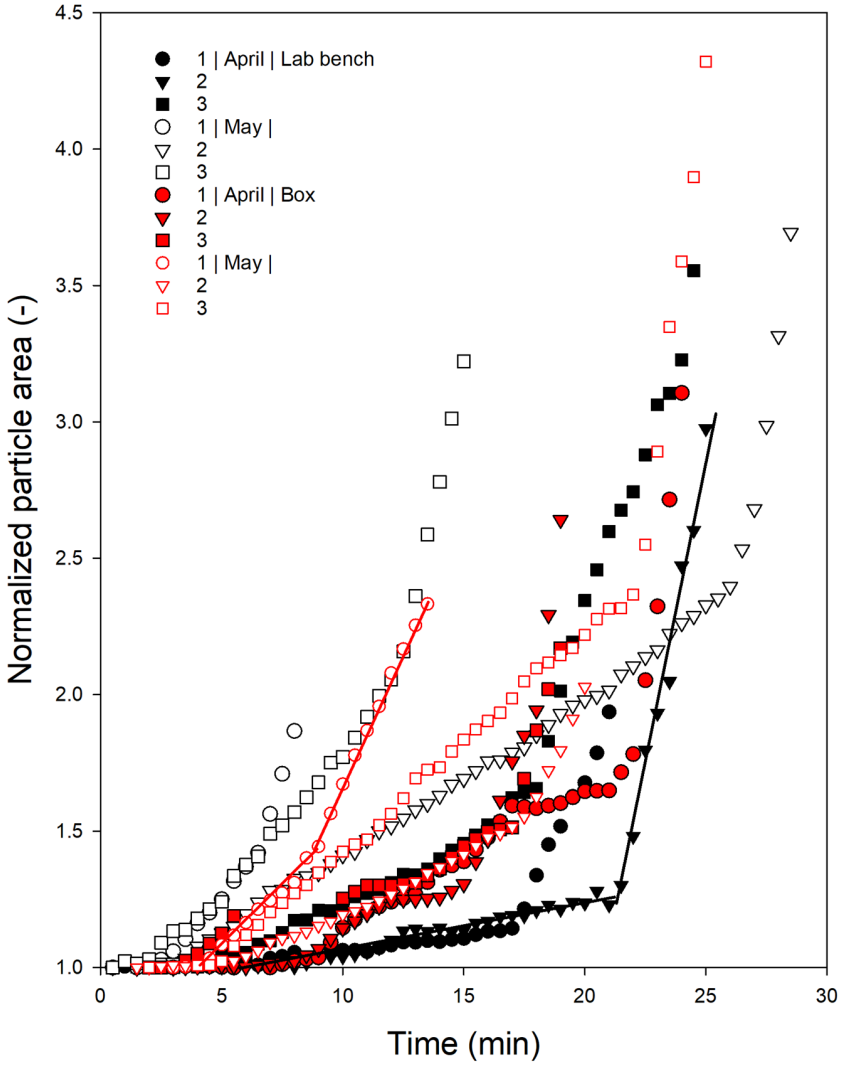

Figure 5. Influence of the film drying method and month of the drying experiment on the change in the normalized particle area of CMPs during swelling at T = 20 °C, pH 11.

Figure 6 shows the simulation results and measured data using the example of a single swelling curve from Figure 5. Figure 6a shows how both volume flows change as a function of time in order to illustrate the two-step, linear expansion of the particle area and the characteristic kink in between. After approx. 300 s, the volume flow rate Flow 1 belonging to the first swelling step starts abruptly at approx. 1.7 fL/s. The trigger for this is the step function with the characteristic time, *time1* for the corresponding rate coefficient *RC1* (Figure 6b, bottom). Within the next 700 s, Flow 1 increases slightly over-proportionally up to a level of 3.2 fL/s. This describes the increase in particle area during the first swelling step until the second step begins after approx. 1100 s. Previous studies have shown that the first swelling step is strongly calcium dependent and thus affects both the charge state of the caseins and the electrostatic contacts, in particular the various forms of calcium phosphate contacts [5], between the caseins. Even small amounts of added calcium (0.1 mM) slow down the rate of the first swelling step or stabilize the CMPs from 1 mM in such a way that a plateau forms before the second swelling step begins [28]. By adding 10 mM calcium, the swelling process could be almost completely suppressed. In contrast, the calcium chelator citrate accelerates the first swelling process and leads to increased SDS decomposition

rates of the CMPs [37]. The stabilizing effect of calcium is based on the suppression of electrostatic repulsion, which occurs because of the deprotonation of glutamic and aspartic acid within the casein chains after a pH shift to alkaline [6]. Furthermore, a reduced proportion of ions in the medium leads to dissociation and swelling, which is suppressed by the added salt [38].

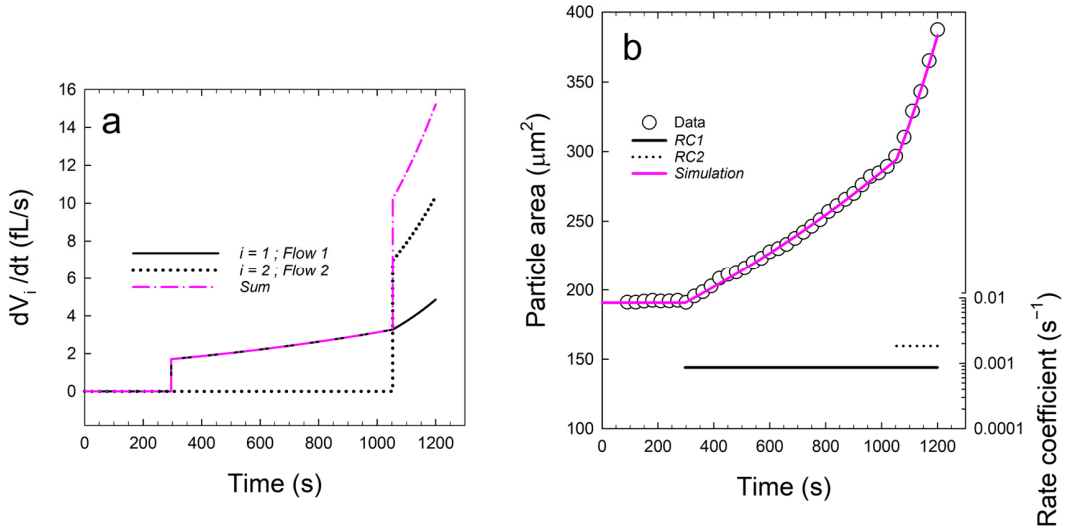

Figure 6. Analysis of a swelling curve shown in Figure 5 using the system dynamics model (Figure 3). (**a**) Temporal change in the simulated total volume flow, which is composed of the volume flows Flow 1 and Flow 2. (**b**) Measured absolute particle size and simulation, as well as step functions for the rate coefficients *RC1* and *RC2*.

In contrast, citrate chelates calcium in the soluble phase and thus indirectly demineralizes casein micelles [39,40]. As a result, the phoshoseryl clusters of the caseins in particular become negatively charged, which promotes water binding and thus swelling. Indirectly, hydrophobic interactions between the caseins are also weakened, which explains the increased SDS decomposition rates after the addition of citrate.

The results indicate that the internal microstructure of the CMPs expands during the first swelling step. These µm sized building blocks consist of several casein micelles covered by a κ-casein surface layer. However, there is not enough κ-casein available to completely cover micellar surfaces [41]. It is plausible that contact between the aggregates within the CMPs occurs via hydrophobic contact surfaces, similar to what has been proposed for individual casein micelles under natural conditions as a reason for the formation of 1-dimensional aggregates [42,43]. As the second swelling step shows no dependence on citrate ions [37], it can be assumed that there are no calcium phosphate contacts between the aggregates of the microstructure.

In the swelling curve shown in Figure 6b, the dissociation of the swollen aggregates starts at the kink point after approx. 1000 s. The instantaneous change in the slope in Figure 6b requires a jump in the total volume flow sum (Figure 6a). This is caused by the second volume flow, Flow 2, which is triggered by the step function of the rate coefficient *RC2* at the characteristic time, *time2*, and increases overproportionally from 7 fL/s after 1050 s to 10.3 fL/s after 1200 s.

We analyzed all the swelling data shown in Figure 5 with the system dynamics model. Figure 7 compares the simulation results for the CMPs dried on the laboratory bench (black symbols) and in the drying apparatus (red symbols). For the six swelling curves per drying method, the rate coefficients are plotted as a function of the characteristic time of the respective swelling step. For the individual CMPs, the rates of the second swelling step are always larger than those of the first step, which has been observed previously [35]. To illustrate the variability of the simulation results, we have connected extreme values of

the population as a polygon. The data for both drying methods scatter similarly for the second swelling step, while there are clear differences for swelling step 1. The data for the first swelling step belonging to film drying in the apparatus form a very narrow cluster with rate coefficients around 10^{-3} s^{-1} and 300 s as the characteristic time. In contrast, the corresponding values for CMPs dried on the bench are much more broadly distributed. We observe CMPs that swell at a rate of 2×10^{-3} s^{-1} after just a short time (100 s). However, we only observe this fast and strong swelling for CMPs that were dried in May. In contrast, CMPs that swell very slowly at rates in the range of $3-9 \times 10^{-4}$ s^{-1} were prepared in April. For CMPs dried in the box, we found a similar but less pronounced trend. The reduced swelling properties of CMPs can be explained by a denser internal structure. Casein micelles are in close contact and their κ-casein surface layers largely overlap [23]. Both the solvent transport through the channels of the inner network and the swelling of the microstructure are then restricted, which explains the delayed start time and the lower rate for the first swelling step. These structural changes can be caused, for example, by hydrophobic collapse due to the temperature post-treatment [44]. In contrast, less compaction of the CMPs leads to improved swelling properties. The casein micelles within the µm sized building blocks are then more loosely packed, resulting in a more porous network structure. If the micellar structure of temperature-treated CMPs is stabilized, e.g., by disulfide bridges, and hydrophobic collapse is thus prevented, correspondingly shorter start times and higher swelling rates are observed [29,44].

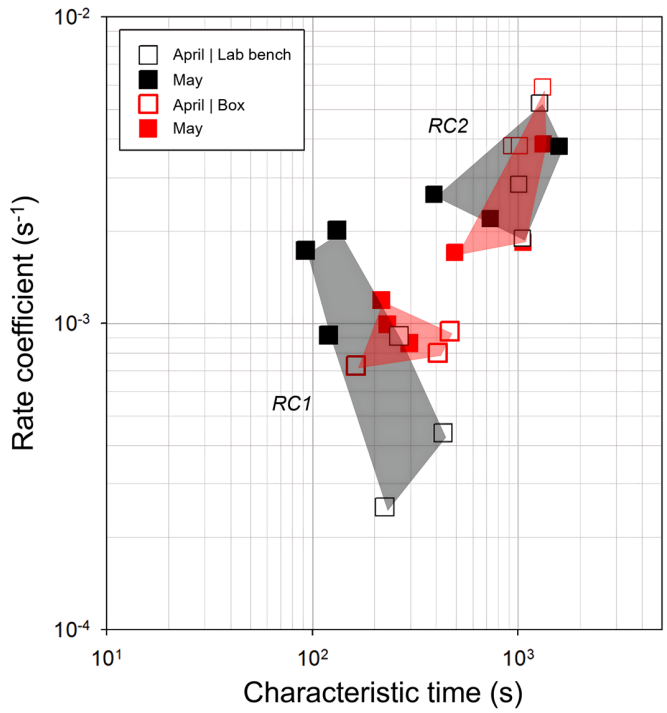

Figure 7. Simulation results for the swelling experiments of CMPs prepared in films on the laboratory bench (white symbols) and in the drying box (red). The variations of the parameter values for process 1 and process 2 are indicated by polygons connecting the extreme values.

Table 1 shows the average air humidity and fluctuations calculated from the values recorded during the last seven hours of drying. In Aachen (Coordinates: 50°46′32″ N 06°05′01″ E), the humidity increases in spring.

Table 1. Mean values and standard deviations of the relative humidity (calculated from the sensor values of the last 7 h of drying—see the gray marked area in Figure 4).

Time of Drying	Drying Method	Mean Value (%)	Standard Deviation (%)
April 2024	Box	40.77	0.96
	Lab bench	31.35	1.18
May 2024	Box	59.15	3.74
	Lab bench	49.54	3.85

During the measurement in April, the average humidity on the laboratory bench was 31.35% and in the drying box was 40.77%. In May, the values were correspondingly higher at 49.54% and 59.15%. The lower humidity in April leads to better drying and more solidified CMPs. The building blocks are then less porous, because the casein micelles are more tightly packed. This slows down the swelling of the caseins and leads to small values for *RC1* for the drying box and laboratory bench (open symbols, Figure 7). However, the values of *RC1* for all dryings in the box are more evenly distributed than those obtained after drying on the laboratory bench. This is shown by a comparison of the red and black polygon areas in Figure 7, which connect the extreme values. The trend can also be observed in the values for drying only in April (open symbols) or only in May (closed symbols).

The distribution of the first swelling rate can be correlated with the variation in humidity. If the measured humidity values are analyzed after the film has formed (i.e., 5 h after the start of drying), the standard deviations for drying in the box are always smaller than on the laboratory bench (compare the values in Table 1). The greater fluctuations in humidity on the laboratory bench can be explained by the movement of people through the laboratory door to the non-air-conditioned floor corridor. Outside the laboratory, the humidity levels were significantly different, as shown by the comparison of the measurements in the laboratory with the humidity data from the local weather station (Figure 4).

Previous studies have shown that casein absorbs moisture quickly in the film state and that the mechanical properties are extremely sensitive to fluctuations in humidity [31]. Although many of the properties were reversible, it sometimes took several hours for them to return to the initial value after humidity correction [32]. Fluctuations in humidity can have a significant influence on the internal structuring of the CMPs. The irregular water absorption and release of the caseins changes the conditions in the film when compaction takes place. While a lack of water leads to denser structures with reduced swelling properties, wetter regions could lead to CMPs with more porous building blocks and better swelling properties. It can therefore be assumed that a more uniform drying process with less fluctuation in humidity results in a more homogeneous compaction of the CMPs with more uniform swelling properties.

4. Conclusions

The swelling process of the CMPs is influenced by the drying conditions, in particular by the average humidity and its fluctuations during the film drying phase. The fluctuations in humidity could be significantly reduced by the drying apparatus described here, consisting of a humidifier and fan system. However, the absolute value of the air humidity is still dependent on the air humidity in the laboratory, which varies greatly depending on the time of day and the season. Drying at lower humidity levels leads to CMPs swelling at a reduced rate. This can be explained by a more compact internal microstructure, which is the result of denser packing of the casein micelles. The more stable humidity in the drying apparatus resulted in CMPs that showed more uniform swelling compared to those drying on the laboratory bench. The system dynamics analysis of the swelling process showed that the variation in the rate of the first swelling step decreased, while there were no changes in the second rate. According to our current knowledge, the first swelling step is caused by the expansion of the inner, granular microstructure of the CMPs, which is interspersed with water channels. The fact that drying under less fluctuating humidity conditions leads to

CMPs with a uniform internal microstructure would be a plausible explanation for similar rates of the first swelling step. In the future, high-resolution imaging techniques should be used to verify this hypothesis. Furthermore, the drying apparatus could be improved to allow drying at different temperatures and humidities under controlled conditions. Moisture sorption isotherms could help to optimize the drying process of the films in the future and to better understand the solidification process of the CMPs. We currently see no alternatives to film drying that guarantee the stabilization of the fragile casein aggregates. Shear forces during spray drying and strong heat flows during freeze and vacuum drying would further restrict the formation conditions of the depletion reaction and impair the stabilization of the fragile casein aggregates.

Author Contributions: Conceptualization, C.H. and R.G.; methodology, C.H. and R.G.; validation, C.H. and R.G., formal analysis, R.G.; investigation, C.H.; resources, R.G.; data curation, C.H. and R.G.; writing—R.G. and C.H.; writing—review and editing, C.H. and R.G.; visualization, C.H. and R.G.; supervision, R.G. All authors have read and agreed to the published version of the manuscript.

Funding: This research received no external funding.

Data Availability Statement: Data are contained within the article.

Acknowledgments: We thank Md Asaduzzaman for helpful discussions. The support of Céline Bastard and Silvia Centeno Benigno (both DWI Aachen) in carrying out the optical data acquisition on the confocal microscope and their constructive discussions are gratefully acknowledged.

Conflicts of Interest: The authors declare no conflicts of interest.

References

1. Holt, C.; Sawyer, L. Caseins as Rheomorphic Proteins: Interpretation of Primary and Secondary Structures of the α S1-, β-and κ-Caseins. *J. Chem. Soc. Faraday Trans.* **1993**, *89*, 2683–2692. [CrossRef]
2. De Kruif, C.G. The Structure of Casein Micelles: A Review of Small-Angle Scattering Data. *J. Appl. Crystallogr.* **2014**, *47*, 1479–1489. [CrossRef]
3. Nascimento, L.G.L.; Casanova, F.; Silva, N.F.N.; de Carvalho Teixeira, A.V.N.; de Carvalho, A.F. Casein-based Hydrogels: A Mini-review. *Food Chem.* **2020**, *314*, 126063. [CrossRef] [PubMed]
4. De Kruif, C.G.; Huppertz, T.; Urban, V.S.; Petukhov, A.V. Casein Micelles and their Internal Structure. *Adv. Colloid Interface Sci.* **2012**, *171*, 36–52. [CrossRef]
5. Hindmarsh, J.P.; Watkinson, P. Experimental Evidence for Previously Unclassified Calcium Phosphate Structures in the Casein Micelle. *J. Dairy Sci.* **2017**, *100*, 6938–6948. [CrossRef]
6. Liu, Y.; Guo, R. PH-dependent Structures and Properties of Casein Micelles. *Biophys. Chem.* **2008**, *136*, 67–73. [CrossRef] [PubMed]
7. De Kruif, C.G.; Zhulina, E.B. κ-Casein as a Polyelectrolyte Brush on the Surface of Casein Micelles. *Colloids Surf. A Physicochem. Eng. Asp.* **1996**, *117*, 151–159. [CrossRef]
8. Bouchoux, A.; Gésan-Guiziou, G.; Pérez, J.; Cabane, B. How to Squeeze a Sponge: Casein Micelles under Osmotic Stress, a SAXS Study. *Biophys. J.* **2010**, *99*, 3754–3762. [CrossRef]
9. Gebhardt, R.; Kulozik, U. Simulation of the Shape and Size of Casein Micelles in a Film State. *Food Funct.* **2014**, *5*, 780–785. [CrossRef] [PubMed]
10. Morris, G.A.; Foster, T.J.; Harding, S.E. Further Observations on the Size, Shape, and Hydration of Casein Micelles from Novel Analytical Ultracentrifuge and Capillary Viscometry Approaches. *Biomacromolecules* **2000**, *1*, 764–767. [CrossRef]
11. Huppertz, T.; Gazi, I.; Luyten, H.; Nieuwenhuijse, H.; Alting, A.; Schokker, E. Hydration of Casein Micelles and Caseinates: Implications for Casein Micelle Structure. *Int. Dairy J.* **2017**, *74*, 1–11. [CrossRef]
12. Tang, C.H. Assembly of Food Proteins for Nano-encapsulation and Delivery of Nutraceuticals (a mini-review). *Food Hydrocoll.* **2021**, *117*, 106710. [CrossRef]
13. Głąb, T.K.; Boratyński, J. Potential of Casein as a Carrier for Biologically Active Agents. *Top. Curr. Chem.* **2017**, *375*, 1–20. [CrossRef] [PubMed]
14. Acuña-Avila, P.E.; Cortes-Camargo, S.; Jiménez-Rosales, A. Properties of Micro and Nano Casein Capsules Used to Protect the Active Components: A Review. *Int. J. Food Prop.* **2021**, *24*, 1132–1147. [CrossRef]
15. Le Goff, G.C.; Srinivas, R.L.; Hill, W.A.; Doyle, P.S. Hydrogel Microparticles for Biosensing. *Eur. Polym. J.* **2015**, *72*, 386–412. [CrossRef] [PubMed]
16. Milenkova, S.; Pilicheva, B.; Uzunova, Y.; Yovcheva, T.; Marudova, M. Casein Microgels as Benzydamine Hydrochloride Carriers for Prolonged Release. *Materials* **2022**, *15*, 1333. [CrossRef] [PubMed]
17. Gasmi, H.; Danede, F.; Siepmann, J.; Siepmann, F. Does PLGA microparticle swelling control drug release? New insight based on single particle swelling studies. *J. Control. Release* **2015**, *213*, 120–127. [CrossRef] [PubMed]

18. Zhuang, Y.; Sterr, J.; Kulozik, U.; Gebhardt, R. Application of Confocal Raman Microscopy to Investigate Casein Micro-particles in Blend Casein/pectin Films. *Int. J. Biol. Macromol.* **2015**, *74*, 44–48. [CrossRef]
19. Maroziene, A.; De Kruif, C.G. Interaction of Pectin and Casein Micelles. *Food Hydrocoll.* **2000**, *14*, 391–394. [CrossRef]
20. Zhang, H.; Goff, H.D.; Liu, C.; Luo, S.; Hu, X. Preparation of Liquid Yogurt in the Presence of Pectin and its Formation Mechanism. *Food Chem.* **2024**, *452*, 139473. [CrossRef]
21. Schulte, J.; Stöckermann, M.; Gebhardt, R. Influence of PH on the Stability and Structure of Single Casein Microparticles. *Food Hydrocoll.* **2020**, *105*, 105741. [CrossRef]
22. Bouchoux, A.; Cayemitte, P.E.; Jardin, J.; Gésan-Guiziou, G.; Cabane, B. Casein Micelle Dispersions under Osmotic Stress. *Biophys. J.* **2009**, *96*, 693–706. [CrossRef] [PubMed]
23. Dahbi, L.; Alexander, M.; Trappe, V.; Dhont, J.K.G.; Schurtenberger, P. Rheology and Structural Arrest of Casein Suspensions. *J. Colloid Interface Sci.* **2010**, *342*, 564–570. [CrossRef] [PubMed]
24. Baracat, M.M.; Nakagawa, A.M.; Casagrande, R.; Georgetti, S.R.; Verri, W.A.; de Freitas, O. Preparation and Characterization of Microcapsules Based on Biodegradable Polymers: Pectin/Casein Complex for Controlled Drug Release Systems. *AAPS Pharmscitech* **2012**, *13*, 364–372. [CrossRef] [PubMed]
25. Vaucher, A.C.D.S.; Dias, P.C.; Coimbra, P.T.; Costa, I.D.S.M.; Marreto, R.N.; Dellamora-Ortiz, G.M.; De Freitas, O.; Ramos, M.F. Microencapsulation of Fish Oil by Casein-Pectin Complexes and Gum Arabic Microparticles: Oxidative Stabilisation. *J. Microencapsul.* **2019**, *36*, 459–473. [CrossRef]
26. Heidebach, T.; Först, P.; Kulozik, U. Influence of Casein-Based Microencapsulation on Freeze-Drying and Storage of Probiotic Cells. *J. Food Eng.* **2010**, *98*, 309–316. [CrossRef]
27. Würth, R.; Lonfat, J.; Kulozik, U. Gelation of Pre-renneted Milk Concentrate during Spray Drying and Rehydration for Microcapsule Formation. *Food Bioprocess Technol.* **2019**, *12*, 211–219. [CrossRef]
28. Schulte, J.; Stöckermann, M.; Thill, S.; Gebhardt, R. Calcium Effect on the Swelling Behaviour and Stability of Casein Microparticles. *Int. Dairy J.* **2020**, *105*, 104692. [CrossRef]
29. Asaduzzaman, M.; Gebhardt, R. Influence of Post-Treatment Temperature on the Stability and Swelling Behavior of Casein Microparticles. *Macromol. Mater. Eng.* **2023**, *308*, 2200661. [CrossRef]
30. Devi, S.; Chaturvedi, M.; Fatima, S.; Priya, S. Environmental Factors Modulating Protein Conformations and their Role in Protein Aggregation Diseases. *Toxicology* **2022**, *465*, 153049. [CrossRef]
31. Bonnaillie, L.M.; Zhang, H.; Akkurt, S.; Yam, K.L.; Tomasula, P.M. Casein Films: The Effects of Formulation, Environmental Conditions and the Addition of Citric Pectin on the Structure and Mechanical Properties. *Polymers* **2014**, *6*, 2018–2036. [CrossRef]
32. Bonnaillie, L.M.; Tomasula, P.M. Application of Humidity-controlled Dynamic Mechanical Analysis (DMA-RH) to Moisture-sensitive Edible Casein Films for Use in Food Packaging. *Polymers* **2015**, *7*, 91–114. [CrossRef]
33. Dumpler, J.; Kieferle, I.; Wohlschläger, H.; Kulozik, U. Milk Ultrafiltrate Analysis by Ion Chromatography and Calcium Activity for SMUF Preparation for Different Scientific Purposes and Prediction of its Supersaturation. *Int. Dairy J.* **2017**, *68*, 60–69. [CrossRef]
34. De Kruif, C.G.; Tuinier, R. Polysaccharide Protein Interactions. *Food Hydrocoll.* **2001**, *15*, 555–563. [CrossRef]
35. Schulte, J.; Pütz, T.; Gebhardt, R. Statistical Analysis of the Swelling Process of Casein Microparticles Based on Single Particle Measurements. *Food Hydrocoll. Health* **2021**, *1*, 100014. [CrossRef]
36. Roche, J.; Caro, J.A.; Norberto, D.R.; Barthe, P.; Roumestand, C.; Schlessman, J.L.; Garcia, A.E.; García-Moreno, B.; Royer, C.A. Cavities Determine the Pressure Unfolding of Proteins. *Proc. Natl. Acad. Sci. USA* **2012**, *109*, 6945–6950. [CrossRef] [PubMed]
37. Asaduzzaman, M.; Pütz, T.; Gebhardt, R. Citrate Effect on the Swelling Behaviour and Stability of Casein Microparticles. *Sci. Rep.* **2022**, *12*, 18401. [CrossRef] [PubMed]
38. Vaia, B.; Smiddy, M.A.; Kelly, A.L.; Huppertz, T. Solvent-mediated Disruption of Bovine Casein Micelles at Alkaline PH. *J. Agric. Food Chem.* **2006**, *54*, 8288–8293. [CrossRef] [PubMed]
39. Broyard, C.; Gaucheron, F. Modifications of Structures and Functions of Caseins: A Scientific and Technological Challenge. *Dairy Sci. Technol.* **2015**, *95*, 831–862. [CrossRef]
40. McCarthy, N.A.; Power, O.; Wijayanti, H.B.; Kelly, P.M.; Mao, L.; Fenelon, M.A. Effects of Calcium Chelating Agents on the Solubility of Milk Protein Concentrate. *Int. J. Dairy Technol.* **2017**, *70*, 415–423. [CrossRef]
41. Dalgleish, D.G. The Basis of Structure in Dairy-based Foods: Casein Micelles and their Properties. In *Food Structures, Digestion and Health*; Boland, M., Golding, M., Singh, H., Eds.; Elsevier: Amsterdam, The Netherlands, 2014; pp. 83–105. [CrossRef]
42. Pink, D.A.; Peyronel, F.; Quinn, B.; Marangoni, A.G. Spontaneous Aggregation of Bovine Milk Casein Micelles: Ultra-small Angle X-ray Scattering and Mathematical Modeling. *Phys. Fluids* **2019**, *31*, 077105. [CrossRef]
43. Takagi, H.; Nakano, T.; Aoki, T.; Tanimoto, M. A SAXS and USAXS Study of the Influence of PH on the Casein Micelle Structure. *Food Chem.* **2024**, *443*, 138606. [CrossRef] [PubMed]
44. Gebhardt, R.; Hohn, C.; Asaduzzaman, M. Stabilizing Interactions of Casein Microparticles after a Thermal Post-treatment. *Food Chem.* **2024**, *450*, 139369. [CrossRef] [PubMed]